

Research Article

# Similar phylogeographic history in a fig species and its obligate pollinators forms parallel genetic structure

Min Liu<sup>1,2,†, ID</sup>, Man-Juan Huang<sup>2,†</sup>, Finn Kjellberg<sup>3</sup>, Yan Chen<sup>4</sup>, Jian Zhang<sup>2,5</sup>, Rui Zhao<sup>2</sup>, Yuan-Yuan Ding<sup>2</sup>, Yang Yang<sup>2</sup>, Jun-Yin Deng<sup>2</sup>, Kai Jiang<sup>2,6, ID</sup>, Yuan-Yuan Li<sup>2</sup>, Xin Tong<sup>2</sup>, Tong Luo<sup>2</sup>, Rong Wang<sup>2,7,\*, ID</sup> and Xiao-Yong Chen<sup>2,7,\*, ID</sup>

<sup>1</sup>School of Life Sciences, Guangzhou University, Guangzhou 510006, China, <sup>2</sup>Zhejiang Tiantong Forest Ecosystem National Observation and Research Station, School of Ecological and Environmental Sciences, East China Normal University, Shanghai 200241, China, <sup>3</sup>CEFE, CNRS, University of Montpellier, EPHE, IRD, Montpellier 34293, France, <sup>4</sup>Ecological Security and Protection Key Laboratory of Sichuan Province, Mianyang Normal University, Mianyang 621000, China, <sup>5</sup>Zhongfu Information Corporation, Jinan 250101, China, <sup>6</sup>Shanghai Chenshan Plant Science Research Center, Chinese Academy of Sciences, Chenshan Botanical Garden, Shanghai 201602, China, <sup>7</sup>Shanghai Institute of Pollution Control and Ecological Security, Shanghai 201403, China

\*Corresponding author. E-mail: [rwang@des.ecnu.edu.cn](mailto:rwang@des.ecnu.edu.cn) (R.W.); [xychen@des.ecnu.edu.cn](mailto:xychen@des.ecnu.edu.cn) (X.-Y.C.)

†These authors contributed equally to this work.

**Handling Editor:** Shucun Sun

**Received:** 5 September 2024, **First Decision:** 22 November 2024, **Accepted:** 30 December 2024, **Online Publication:** 13 January 2025

**Citation:** Liu Min, Huang Man-Juan, Kjellberg Finn, Chen Yan, Zhang Jian, Zhao Rui, Ding Yuan-Yuan, Yang Yang, Deng Jun-Yin, Jiang Kai, Li Yuan-Yuan, Tong Xin, Luo Tong, Wang Rong, Chen Xiao-Yong (2025) Similar phylogeographic history in a fig species and its obligate pollinators forms parallel genetic structure. *J Plant Ecol* 18:rtaf007. <https://doi.org/10.1093/jpe/rtaf007>

## Abstract

Closely related and co-distributed species usually share a common phylogeographic history, but it remains unclear whether ecologically interacting species can respond synchronously to historical climate changes. Here, we focused on a fig–pollinator mutualism comprising *Ficus pumila* var. *pumila* and its obligate pollinators (morphospecies *Wiebesia pumilae*), and collected samples across most of their distribution ranges. We employed cytoplasmic DNA sequences and nuclear microsatellite loci to reveal the species composition within the pollinators and to test whether the two mutualists exhibited similar postglacial phylogeographic patterns. We identified three cryptic pollinator species, with two dominant cryptic species exhibiting parapatric distributions in the northern and southern parts of the plant's range, respectively. Similar current spatial genetic structures were detected in the two dominant cryptic pollinator species and the host plant, with both showing eastern and western genetic clusters. Moreover, evidence for postglacial expansion was found for all three species, and their potential refugia during the Last Glacial Maximum were located in the eastern and western parts of their distribution ranges. These results suggest synchronous responses to historical climate changes. Our study demonstrates congruent phylogeographic patterns between obligate mutualists and highlights the role of biogeographic factors in shaping the current biodiversity across trophic levels.

**Keywords:** comparative phylogeography, cryptic species, fig–pollinator mutualisms, glacial refugia, population expansion

## 薜荔与其传粉小蜂间相似的亲缘地理史形成平行的遗传结构

**摘要:**分布相同且紧密相关的物种通常具有相似的亲缘地理历史,然而相互作用物种是否对历史气候变化表现出同步响应仍不清晰。本研究聚焦于薜荔(*Ficus pumila* var. *pumila*)及其专性传粉小蜂(形态种:薜荔传粉小蜂*Wiebesia pumilae*)组成的互惠共生体系,从它们分布范围内广泛取样,采用胞质DNA序列和核微卫星标记分析传粉小蜂物种组成,并检验薜荔及其传粉小蜂是否呈现相似的冰期后亲缘地理格局。我们在传粉小蜂中发现了3个隐存种,其中2个优势隐存种分别位于薜荔的北部和南部分布区,且总体呈异域分布。这2个优势隐存种与其宿主植物具有相似的空间遗传结构,均可划分出东、西2个遗传类群。此外,薜荔与这2个传粉小蜂隐存种在分布范围的东部和西部均存在末次冰盛期的潜在避难所,并表现出冰期后扩张的信号。上述结果表明,薜荔与其专性传粉小蜂对历史气候变化的响应具有同步性。本研究揭示了专性互惠共生物种间一致的亲缘地理格局,强调了生物地理因素在塑造不同营养级现存生物多样性格局中的重要作用。

**关键词:**比较亲缘地理,隐存种,榕-蜂互惠共生关系,冰期避难所,种群扩张

## INTRODUCTION

Historical biogeographic factors can affect speciation, extinction and migration, and ecological interactions maintaining the coexistence of species (Bansal *et al.* 2022; Lu *et al.* 2018; Yin *et al.* 2023). In the subtropical and temperate zones of Eurasia, Pleistocene climatic oscillations, especially the Last Glacial Period, have profound effects on current species distribution (Hewitt 2000; Jiang *et al.* 2021, 2024; Tong *et al.* 2022). Many closely related and co-distributed species show concordant historical demographic dynamics and migration trajectories as they often have similar life history characteristics and might synchronously respond to past climate changes (Fu *et al.* 2024; Kreger *et al.* 2020; Marske *et al.* 2020). Such consistent phylogeographic patterns help to understand the formation of current biodiversity pattern at a single trophic level. However, ecosystems are composed of species linked by interspecific interactions across different trophic levels (Akesson *et al.* 2021; Lan *et al.* 2022; Thrall *et al.* 2007; Wang *et al.* 2023). The impacts of historical events on the current distribution of tightly interacting species with long coevolution history may be similar, causing consistent phylogeography (Garrick *et al.* 2013; Yu and Nason 2013). Nevertheless, this hypothesis has seldomly been tested.

There are only a few comparative phylogeographic studies involving interacting species at different trophic levels, but they exhibited distinct results. For example, the white campion (*Silene latifolia*) and its pollinating moth *Hadena bicruris* showed incongruent phylogeographic patterns (Magalhaes *et al.* 2011), but striking similarities in genetic structuring have been

found in some parasites and their hosts (Bothma *et al.* 2021) and in some plants and their pollinating insects (Tian *et al.* 2015). Such an inconsistent phylogeographic patterns of associates may be explained by coevolutionary constraints, host shifts, disintegration of interactions during glacial periods and utilization of different refugia due to differences in adaptative strategies (Althoff *et al.* 2012; Maron *et al.* 2019). Taken together, these reasons reflect the importance of specificity in determining the degree of phylogeographic matching. When interacting species exhibit high specificity, pollinators have little chance to shift to other host plants, and thus they must follow their specific hosts and results in shared responses to historical climatic events. We thus hypothesize that specialized obligate mutualists are highly likely to share postglacial phylogeographic history.

Nevertheless, different current genetic structure has also been recorded in some obligate mutualisms (Deng *et al.* 2020; Liu *et al.* 2013). This is likely caused by distinct dispersal ability between mutualists, leading to asynchronous expansions from refugia (Liu *et al.* 2015; Yu *et al.* 2019). Obligatory pollination mutualisms are one of the most appropriate systems (Liu *et al.* 2013; Yu *et al.* 2019), but even in these mutualisms, the migration of pollinators only represent the pollen movements of their host plants. Furthermore, the causes of genetic structure may be more complicated when multiple obligate pollinators pollinate a single host plant species. Such complicated genetic structure has been documented in several systems, including figs and fig wasps (Deng *et al.* 2023; Yang *et al.* 2015; Yu *et al.* 2019), yuccas and

yucca moths (Godsøe *et al.* 2008), globeflowers and globeflower flies (Després *et al.* 2002; Espíndola *et al.* 2014), and *Silene* and *Hadena* (Kephart *et al.* 2006). In this case, it is crucial to describe the composition of pollinators and their phylogenetic relationships before comparing phylogeographic patterns.

Fig trees (*Ficus*, Moraceae) and their pollinating wasps (Agaonidae, Hymenoptera) constitute a classic example of obligate mutualism (Weiblen 2002). In a fig–pollinator mutualism, the fig species produces enclosed inflorescences called figs which are pollinated by a unique or only a few pollinating wasp species, whose larvae can only grow in the galled ovules inside host figs (Wang *et al.* 2019; Yang *et al.* 2023). Therefore, these highly specialized mutualisms provide an ideal system for testing our hypothesis. Previous comparative phylogeographic studies on several fig–pollinator mutualisms have revealed conflicting results in the matching degree of phylogeographic patterns (Rodríguez *et al.* 2017; Tian *et al.* 2015; Yu *et al.* 2019), probably due to the differences in time scales and the complicated historical background in tropical zones. The recent phylogeographic history of fig–pollinator mutualisms distributed in subtropical and temperate zones has been poorly explored, despite the well-documented influences of the Last Glacial Period in these regions.

In this study, we chose *Ficus pumila* L. and its pollinating wasps as our study system. *Ficus pumila* is a functionally dioecious creeping fig tree, which is widely distributed in subtropical areas of East Asia (Liu *et al.* 2015). *Wiebesia pumilae* is the host-specific pollinator of *F. pumila*, but molecular studies have evidenced three cryptic species within this morphospecies (Chen *et al.* 2012; Zhang *et al.* 2022), and additional cryptic species may exist as these previous studies only conducted sampling within a limited area in the natural distribution range of *F. pumila*. Moreover, though genetic structure and demography of *F. pumila* and *W. pumilae* had been separately studied (Chen *et al.* 2012; Liu *et al.* 2015), a rigorous comparison (based on pairwise sampling in each location) of genetic structure and population dynamics between these two mutualists across their main natural distribution range has not yet been performed. In this study, we expanded our sampling range to cover most of their distribution areas in China and conducted a comparative phylogeographic study using both nuclear DNA markers and cytoplasmic DNA makers, to answer: 1) How many cryptic pollinator species of *F. pumila* are present in China and what is their distribution pattern? 2) Do *F.*

*pumila* and the pollinators present congruent current spatial genetic structure? and 3) Do *F. pumila* and the pollinators share similar signatures of postglacial expansion?

## MATERIALS AND METHODS

### Study species and sample collection

*Ficus pumila* contains two varieties, *F. pumila* var. *pumila* and *F. pumila* var. *awkeotsang*, while the former has a wide distribution range, the latter occurs part distribution of the species in the southeastern coasts of mainland and Taiwan Island (Liu *et al.* 2015; Wang *et al.* 2013). The three cryptic pollinator species of *F. pumila* (*Wiebesia* sp. 1, 2 and 3) have been reported to have a largely parapatric distribution in southeast China (Chen *et al.* 2012). *Wiebesia* sp. 1 and *Wiebesia* sp. 2 are distributed in south of the Yangtze River in China, with the Nanling and Wuyi Mountains as the main boundary, and *Wiebesia* sp. 3 is an insular species mainly found on some islands nearby the southeastern coast of China (Tong *et al.* 2021). Sympatric occurrence of two cryptic species has been observed in the contact zones (Chen *et al.* 2012).

From 2006 to 2012, we collected leaves of the two varieties of *F. pumila* and their adult pollinating wasps. Our sampling locations covered most distribution range of *F. pumila* in China (Fig. 1a and b). Healthy leaves were collected from each individual of *F. pumila*, and mature females of the pollinator were collected from mature figs. In total, *F. pumila* and the pollinators were sampled from 82 and 76 locations within their natural distribution ranges (Supplementary Table S1). Note that *F. pumila* var. *awkeotsang* samples were only used for constructing phylogenetic trees and were excluded from all analyses of population genetics and phylogeography due to its limited distribution.

### DNA extraction, microsatellite genotyping and cytoplasmic DNA segment sequencing

For *F. pumila*, the total genomic DNA was extracted using the Plant Genomic DNA Kit (Tiangen, Beijing, China). To study its genetic structure, eight nuclear microsatellite loci (*FP9*, *FP38*, *FP102*, *FP134*, *FP213*, *FP540*, *FP556* and *FP601*) were amplified and genotyped as described by Zhang *et al.* (2011). In addition, three non-coding regions of chloroplast DNA (cpDNA) (*trnS–trnG*, *atpF–atpH* and *trnC–ycf6*) were amplified and bidirectionally sequenced as described by Liu *et al.* (2015).

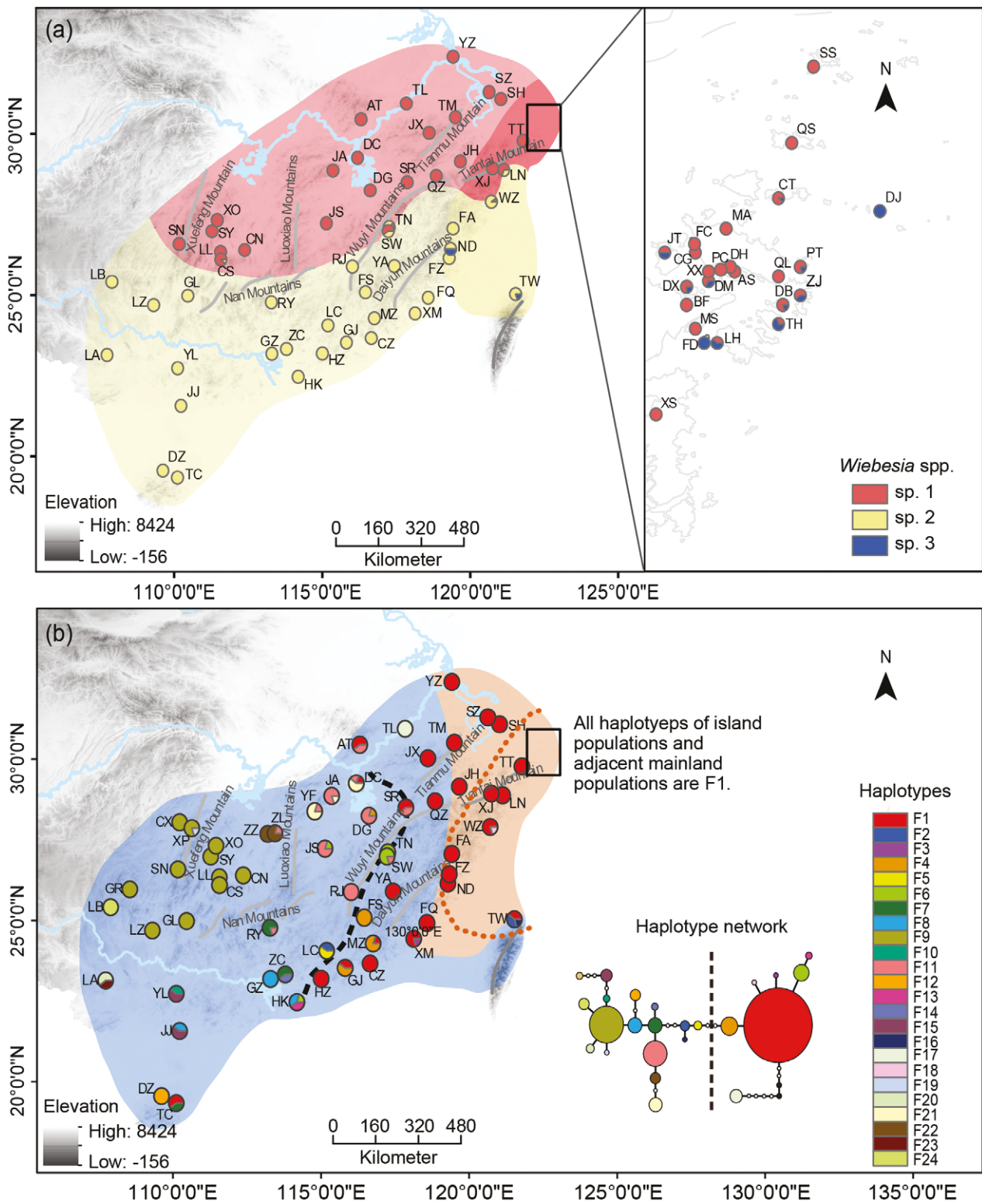


**Figure 1:** Current genetic structure of the three cryptic species in *W. pumilae* (a) and *F. pumila* (b) and their phylogenetic trees (c). The distribution ranges and locations of cryptic species (*Wiebesia* sp. 1, sp. 2 and sp. 3) are represented by red, yellow and blue, and the light and dark red regions as well as the light and dark yellow regions represent different genetic clusters using microsatellite loci (by STRUCTURE) in *Wiebesia* sp. 1 and sp. 2, respectively (see Supplementary Fig. S1a-d) (a). The network of cpDNA haplotypes (indicated by different colors) in *F. pumila* var. *pumila* and the composition of cpDNA haplotypes in each sampling location, with the boundary separating the two genetic clusters based on cpDNA sequences marked by a black dashed line (b). The regions of different genetic clusters using microsatellite loci (by STRUCTURE)

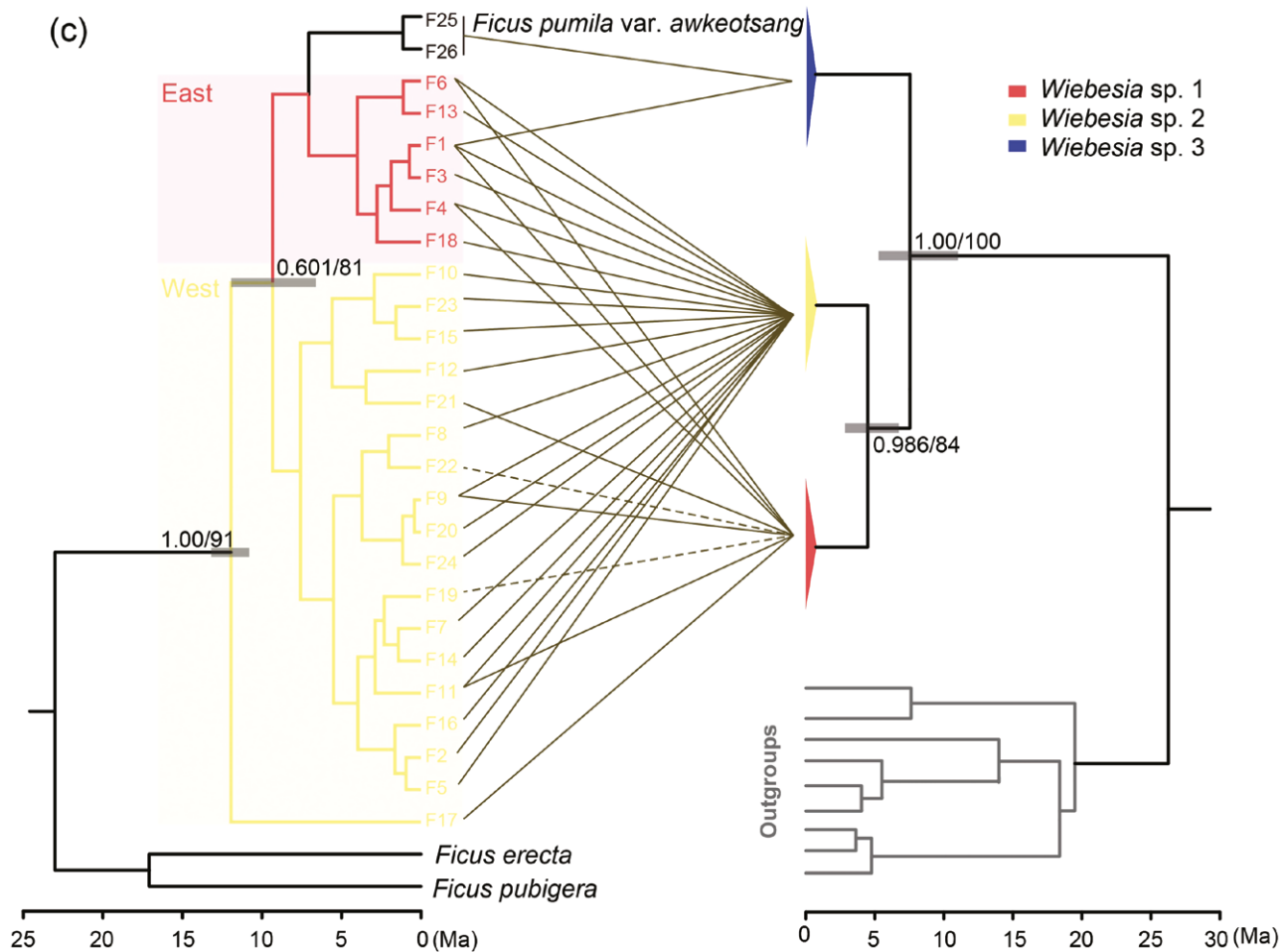


**Figure 1:** Continued

For the pollinators, the total genomic DNA was extracted from each sampled adult female, and genotyping of 10 nuclear microsatellites was conducted as described by [Liu \*et al.\* \(2013\)](#). Mitochondrial DNA (mtDNA) gene *COI* was amplified using the primer pair Jerry/Pat bidirectionally sequenced as described by [Chen \*et al.\* \(2012\)](#).

#### Acquisition of genetic variations and identification of cryptic pollinator species

The sequences of cpDNA and mtDNA fragments were aligned separately using CLUSTALW implemented in MEGA v. 6.06 ([Tamura \*et al.\* 2013](#)). Then, the sequences from different loci were merged together for the following analyses. DnaSP v. 5.10 ([Librado and Rozas 2009](#)) was adopted to calculate the number of haplotypes ( $k$ ), haplotype diversity ( $h$ ) and nucleotide diversity ( $\pi$ ). Haplotype network was analyzed using a statistical parsimony approach implemented in TCS 1.21 ([Clement \*et al.\* 2000](#)). All nodes were connected with a  $>95\%$  probability

cut-off, and K2P (Kimura-2-parameter) distances of sequences were calculated using MEGA v. 6.06.

To assign all pollinating wasps to different cryptic species, we constructed the phylogenetic trees using a series of *COI* sequences of fig wasps as outgroups ([Supplementary Table S2](#)). Two methods were used for reconstructing phylogenetic relationships. First, the maximum likelihood (ML) approach was conducted by PHYML v. 3.0 ([Guindon \*et al.\* 2010](#)). The nucleotide substitution model selected was TVM+I + G, with the starting tree constructed using the maximum parsimony method. The tree topology was estimated using the Subtree Pruning and Regrafting option, and node support was estimated with 100 bootstrap replicates. Second, Bayesian phylogenetic trees were constructed using software BEAST v. 1.8.2 ([Drummond \*et al.\* 2012](#)), using the nucleotide substitution model chosen by JMODELTEST with *COI* data partitioned into two parts (1 + 2, 3) based on codon positions. BEAST was run under a strict clock, with tree prior as Yule process

and MCMC steps as 60 000 000 (sampled every 1000 generations). Log files were checked using TRACER v. 1.7 (Rambaut *et al.* 2018), ensuring the effective sample size for each parameter exceeded 200. The phylogenetic tree was summarized by TreeAnnotator v. 1.8.2 followed by the removal of 10% burn-in. Node ages of the Bayesian tree were estimated and calibrated by the divergence time between genera *Pegoscapus* and *Tetrapus*, with prior age distribution specified by lognormal distribution (mean = 0.9; stev = 0.9; offset = 16; 95% highest posterior density [HPD] = 16.42–30.35 Ma).

For microsatellite loci, linkage disequilibrium (LD) among loci per population and deviation from the Hardy–Weinberg equilibrium (HWE) of each locus in each population were tested using GENEPOP v. 4.0 (Rousset 2008), with false discovery rate correction (Benjamini and Hochberg 1995). The presence of null alleles was detected with MICRO-CHECKER (van Oosterhout *et al.* 2004). We used the following indices calculated by FSTAT v. 2.9.3 (Goudet 1995) and GenALEX v. 6.5 (Peakall and Smouse 2012) to characterize within-population genetic diversity: mean number of alleles per locus ( $N_A$ ), allelic richness per locus ( $A_R$ ), and observed ( $H_o$ ) and unbiased expected heterozygosities ( $H_e$ ). We adopted linear regression to test the correlation of genetic diversity between each cryptic pollinator species and its corresponding host plant populations. Populations with fewer than five samples were excluded from all analyses at the population level.

### Genetic differentiation and isolation by distance

To test whether differentiation between *F. pumila* var. *pumila* populations correlated with that of the pollinators, we calculated the genetic differentiation based on microsatellite loci. We estimated both the overall  $F_{ST}$  value and those between populations and calculated unbiased  $F_{ST}$  ( $F_{ST(ENA)}$ ) using the ENA (excluding null alleles) method in FREENA (Chapuis and Estoup 2007). The significance of overall genetic differentiation values was tested using 1000 permutations, and  $P$  values were adjusted using the Bonferroni correction method.

To evaluate the relative role of pollen dispersal in shaping the genetic differentiation among *F. pumila* var. *pumila* populations, we calculated the pollen-to-seed migration ratio ( $r$ ) for all populations and those pollinated only by *Wiebesia* sp. 1 or *Wiebesia* sp. 2, using estimations of  $F_{ST}$  based on both microsatellite loci and cpDNA sequences as proposed by Ennos (1994). We did not include the populations pollinated

by *Wiebesia* sp. 3 because it appeared in very few locations (Supplementary Table S1).

Then, isolation by distance was evaluated for both plant and pollinator populations using Mantel tests, with  $F_{ST}/(1 - F_{ST})$  or  $F_{ST(ENA)}/(1 - F_{ST(ENA)})$  as the estimates of genetic distances, in R package ‘vegan’ (Oksanen *et al.* 2019), setting 10 000 permutations.

### Genetic clustering

STRUCTURE v. 2.3.1 (Pritchard *et al.* 2000) was used to infer genetic structure for each cryptic pollinator species and *F. pumila* var. *pumila* based on microsatellite loci. We ran the admixture model with correlated frequencies, with 10 independent runs for each  $K$  (from 1 to 10) performed with 1 000 000 MCMC repetitions and a burn-in of 300 000. We used both the mean maximum estimated logarithm of posterior probability LnP(D) (Pritchard *et al.* 2000) and  $\Delta K$  values (Evanno *et al.* 2005) to determine the optimal  $K$ . Assignment probabilities were averaged across all 10 replicate runs for the optimal  $K$ .

To uncover the genetic structure of *F. pumila* var. *pumila* populations based on cpDNA sequences, we constructed ML and Bayesian phylogenetic trees using the same processes as mentioned above. Node ages of the Bayesian tree were estimated based on two secondary calibration points setting normal distribution (Crauad *et al.* 2012; Xu *et al.* 2011): the divergence time between *F. pumila* and other *Ficus* species (mean = 12.0 Ma; stev = 0.6; 95% HPD = 10.82–13.18 Ma) and that between *F. pumila* and *Ficus erecta* (mean = 23 Ma; stev = 0.5; 95% HPD = 22.02–23.98 Ma).

### Population demographic history

The historical effective population size of each cryptic pollinator species was estimated using the Bayesian skyline plot (BSP) method implemented in BEAST. Nucleotide substitution model for each species was specified by JMODELTEST, with uncorrelated exponential relaxed clocks, tree prior as Bayesian skyline and MCMC of 25 000 000 (sampled every 25 000 generations). To convert the estimates scaled by mutation rate to calendar years, we applied the substitution rate of 1.9% per million years as proposed by Lin *et al.* (2008). We did not conduct this analysis for *F. pumila* due to very few haplotypes in its cpDNA sequences (see *Results*).

Mismatch distributions and neutrality tests (Slatkin and Hudson 1991) implemented in ARLEQUIN v. 3.5 (Excoffier and Lischer 2010) were used to infer the historical population expansion of all cryptic

pollinator species and *F. pumila* var. *pumila*. Both sudden expansion and spatial expansion models (Excoffier 2004) were used. The goodness-of-fit of models was tested based on the sum of squared deviations (SSD) with 10 000 bootstrap replicates. For neutrality tests, Tajima's *D* (Tajima 1989) and Fu's *FS* (Fu 1997) were calculated and tested, using 10 000 simulations.

### Potential distribution at the Last Glacial Maximum of the pollinators and *F. pumila* var. *pumila*

Species distribution modeling was explored to reconstruct the potential distribution of the pollinators and *F. pumila* var. *pumila* at the Last Glacial Maximum (LGM). For the two major pollinators, population locations from our field investigation were used as the presence records. The present occurrence information of *F. pumila* var. *pumila* were obtained from our field investigation, Chinese Virtual Herbarium (<https://www.cvh.ac.cn/>) and Global Biodiversity Information Facility (<http://www.gbif.org/>). To avoid spatial autocorrelation of records and artificial spatial clusters of observations, occurrence records were filtered by OccurrenceThinner (Verbruggen 2012). There were 42, 87 and 209 locations for *Wiebesia* sp. 1, *Wiebesia* sp. 2 and *F. pumila* var. *pumila*, respectively.

Current global climate data were downloaded from the WorldClim website (<http://www.worldclim.org>) at 2.5' spatial resolution. Data from both Community Climate System Model (CCSM) (Collins *et al.* 2006) and Model for Interdisciplinary Research on Climate (MIROC) (Hasumi and Emori 2004) were used for estimating the distributions of *F. pumila* var. *pumila* and its pollinating wasps at LGM. Climate attributes of 19 bioclimatic variables at occurrence records were extracted using ArcGIS v.10. The Variance Inflation Factor (VIF) analysis was used to detect multicollinearity between bioclimatic variables using the *vifstep* function in R package usdm (Naimi *et al.* 2014), and bioclimatic variables with the  $VIF > 10$  were excluded. Eight bioclimatic variables (BIO2, BIO3, BIO8, BIO10, BIO13, BIO15, BIO18 and BIO19) were retained to model the current and LGM distribution of the three species.

The software MAXENT 3.3.3k (Phillips and Dudik 2008) was used to generate the potential distribution of the three species using default settings. Ten independent replicates of subsampling procedures with the random test percentage of 20% and the median probabilities were projected onto the current

and LGM climate. The area under the receiver operating characteristic curve (AUC) was used as an indicator of the accuracy of model estimation.

## RESULTS

### Identification of cryptic pollinator species

For the pollinators, 665 mature females from 76 locations were sequenced for the *COI* gene. The lengths of *COI* gene sequences were 906–909 bp, and 123 haplotypes were detected. The results of phylogenetic analysis showed that all samples were assigned to three major clades (Fig. 1c), each of which contained the haplotypes of a single cryptic species from Chen *et al.* (2012). In addition, the mean K2P distances within each clade were 0.70%, 0.62%, and 0.71%, which were far lower than the K2P distances among clades (ranging from 6.55% to 12.13%). These results confirm the presence of three cryptic pollinator species, with 379, 230 and 56 samples belonging to *Wiebesia* sp. 1, sp. 2 and sp. 3, respectively (Supplementary Tables S3–S5). The estimated node ages of Bayesian tree showed that *Wiebesia* sp. 3 diverged from the common ancestors of *Wiebesia* sp. 1 and sp. 2 at about 7.56 Ma (95% HPD: 5.32–10.99 Ma), and the divergence time between *Wiebesia* sp. 1 and sp. 2 was estimated to be c. 4.50 Ma (95% HPD: 2.92–6.71 Ma) (Fig. 1c).

The three cryptic pollinators are mainly parapatric (Fig. 1a), with the Nanling–Wuyi Mountains as the boundary separating *Wiebesia* sp. 1 from *Wiebesia* sp. 2, and *Wiebesia* sp. 3 is mainly distributed in Zhoushan Archipelago, where it is sympatric with *Wiebesia* sp. 1. *Wiebesia* sp. 3 was also found in Ningde and Taiwan Island, where it pollinates *F. pumila* var. *awkeotsang* (Fig. 1c).

### Genetic variations

For the pollinators, we genotyped a total of 1471 mature females using microsatellite loci, with no significant signals of LD. The clustering analysis allocated all samples into three distinct clusters, perfectly matching the distribution of the three cryptic pollinator species inferred from *COI* sequences (Supplementary Fig. S1a). We therefore identified the 802, 507 and 162 samples as *Wiebesia* sp. 1, sp. 2 and sp. 3, respectively. For *F. pumila* var. *pumila*, a total of 1682 samples were genotyped using microsatellite loci, with no significant signals of LD.

In all three cryptic pollinator species and *F. pumila* var. *pumila*, significant deviations from the HWE were

only detected in a few locations for each microsatellite locus, and no evidence of the presence of null alleles were detected in all loci. Values of genetic diversity indices are presented in **Supplementary Tables S1** and **S3–S5**. For the pollinators, there were no significant correlations between genetic diversity and latitude or longitude, and all indices ( $N_A$ ,  $A_R$ ,  $H_E$ ,  $H_O$ ) of *F. pumila* var. *pumila* decreased significantly with increasing latitude and longitude (**Supplementary Fig. S2**).

Using the combination of three cpDNA fragments (a total length of 2413 bp), we obtained a total of 26 haplotypes in *F. pumila* from 407 samples, with two haplotypes specifically associated with *F. pumila* var. *awkeotsang* (**Fig. 1b**; **Supplementary Table S1**). Haplotype diversity ( $h$ ) and nucleotide diversity ( $\pi$ ) for all locations were 0.667 and 0.00122, respectively, and most locations had only one haplotype (**Fig. 1b**; **Supplementary Table S1**).

### Genetic differentiation among populations

For the pollinators, the overall genetic differentiation (using microsatellites) of *Wiebesia* sp. 1, sp. 2 and sp. 3 were 0.118 ( $F_{ST}$ ) and 0.113 ( $F_{ST(ENA)}$ ), 0.078 ( $F_{ST}$ ) and 0.077 ( $F_{ST(ENA)}$ ), and 0.089 ( $F_{ST}$ ) and 0.085 ( $F_{ST(ENA)}$ ) (all  $P$  values  $< 0.05$ ). Significant positive correlations between pairwise genetic differentiation and geographic distance were detected in *Wiebesia* sp. 1 and *Wiebesia* sp. 2 (**Supplementary Fig. S3a–f**).

For *F. pumila* var. *pumila*, the overall genetic differentiation (using microsatellites) was 0.160 ( $F_{ST}$ ) and 0.156 ( $F_{ST(ENA)}$ ) (both  $P$  values  $< 0.05$ ). Mantel tests revealed a significantly positive relationship between genetic differentiation and geographic distance (**Supplementary Fig. S3g and h**). The genetic differentiation based on cpDNA sequences was 0.833, and the pollen-to-seed dispersal ratio ( $r$ ) was 24.19. In addition, the genetic differentiation ( $F_{ST}$ ) among populations of *F. pumila* var. *pumila* pollinated only by *Wiebesia* sp. 1 was 0.169 (microsatellites) and 0.809 (cpDNA), leading to an  $r$  value of 18.83. The  $F_{ST}$  values among the plant populations pollinated by only *Wiebesia* sp. 2 were 0.140 (microsatellites) and 0.799 (cpDNA), with an  $r$  value of 22.42.

### Genetic clustering

For the pollinators, we detected obvious genetic structure in *Wiebesia* sp. 1 and *Wiebesia* sp. 2. All samples of these two cryptic species were assigned into two genetic clusters, i.e. the western cluster containing most samples from inland and some coastal locations and the eastern cluster mainly comprising samples from some coastal locations and nearby islands (**Fig.**

**1a; Supplementary Fig. S1b and c**). There was no clear genetic clustering pattern for *Wiebesia* sp. 3 even for  $K = 2$  (**Supplementary Fig. S1d**). For *F. pumila* var. *pumila*, using microsatellites, two genetic clusters were also detected, with the eastern cluster containing most samples from locations in the northeast of our sampling range and the western cluster containing samples from the rest locations (**Supplementary Fig. S1b and e**).

Interestingly, the combination of the two eastern clusters and that of the two western clusters of the two major cryptic pollinator species roughly matched the ranges of the two clusters of *F. pumila* var. *pumila*, though the boundary of the pollinators slightly shifted eastwards compared with that of the plant (**Fig. 1a and b**). The phylogenetic tree and the haplotype network based on cpDNA haplotypes also showed the presence of the eastern and the western cluster, but the dividing line moved westwards to the Wuyi Mountains (**Fig. 1b and c**).

### Historical demography of the pollinators and *F. pumila* var. *pumila*

Results from BSP analysis showed that the effective population sizes of *Wiebesia* sp. 1 and *Wiebesia* sp. 2 started to increase since about 20 000 years BP and 30 000 years BP but the effective population size of *Wiebesia* sp. 3 began to decrease from about 10 000 BP (**Fig. 2a–c**). Moreover, significant sudden expansion was found in *Wiebesia* sp. 1 and *Wiebesia* sp. 2 but not in *Wiebesia* sp. 3 (**Table 1**). We observed different mismatch distributions among the three cryptic pollinator species. *Wiebesia* sp. 1 and *Wiebesia* sp. 2 exhibited a flat and unimodal peak distribution curve (**Fig. 2d and e**). For *Wiebesia* sp. 3, a sharp decrease in frequency was detected when pairwise differences increased (**Fig. 2f**), indicating a recent bottleneck. In addition, the neutrality tests in *Wiebesia* sp. 1 and sp. 2 also showed evidence for expansions, with both Tajima's  $D$  and Fu's  $Fs$  having negative values though significant results were only detected for Fu's  $Fs$  ( $P < 0.001$ , **Table 1**).

For *F. pumila* var. *pumila*, mismatch distributions using cpDNA sequences under both sudden expansion and spatial expansion models did not reject significant demographic and spatial expansions in the two genetic clusters (**Table 1**). Besides, the observed pairwise differences of these two clusters rapidly decreased to very low values (**Fig. 2g and h**), also suggesting recent expansions. Additionally, negative values were found in Tajima's  $D$  and Fu's  $Fs$  in both clusters, a sign of recent population expansions (**Table 1**).

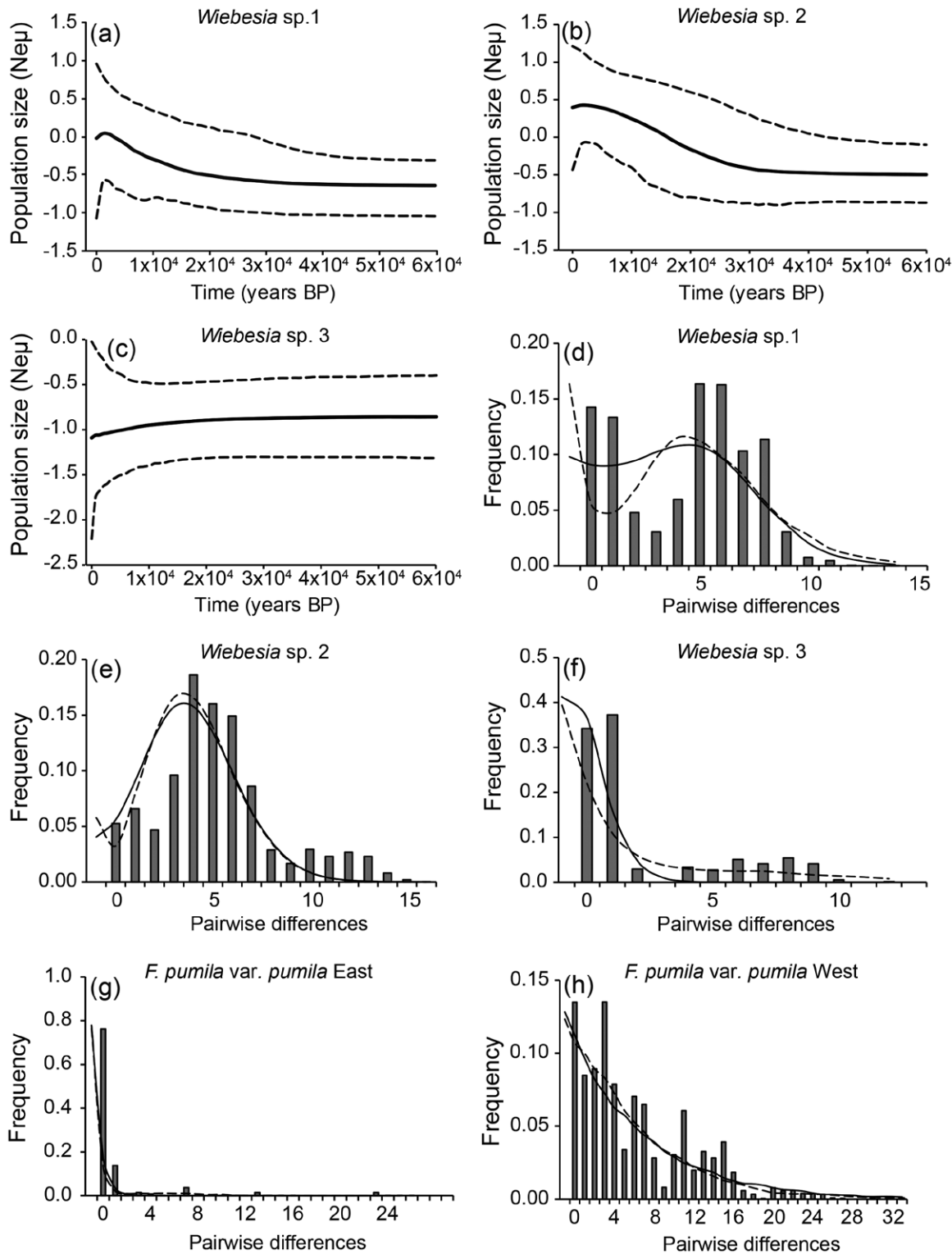


**Figure 2:** Historical demographics of the three cryptic species in *Wiebesia pumila* according to the results from BSP analysis (a-c) and mismatch distribution of each cryptic species (d-f) and *Ficus pumila* var. *pumila* (g, h). In the BSPs, the solid and dashed lines represent the medians of estimates and the higher and lower 95% HPD limits. For mismatch distribution, the gray bars, solid lines and dashed lines show the observed frequency of pairwise differences, the simulated distribution under a sudden expansion model and the expectation under the spatial expansion model, respectively.

**Table 1:** Results of mismatch distribution and neutral tests of the three cryptic species in *Wiebesia pumilae* and *Ficus pumila* var. *pumila*

Species	Mismatch distribution				Neutral test			
	SSD	$P_{(SSD)}$	SSD	$P_{(SSD)}$	Tajima's $D$	$P_{(D)}$	Fu's $Fs$	$P_{(Fs)}$
Cryptic species in <i>W. pumilae</i>								
<i>Wiebesia</i> sp. 1	0.021	0.195	0.019	0.493	-1.052	0.135	-20.71	<b>&lt;0.001</b>
<i>Wiebesia</i> sp. 2	0.008	0.114	0.007	0.277	-1.106	0.118	-25.05	<b>&lt;0.001</b>
<i>Wiebesia</i> sp. 3	0.035	<b>0.042</b>	0.043	0.273	-1.556	<b>0.037</b>	0.076	0.558
<i>F. pumila</i> var. <i>pumila</i>								
East	0.004	0.371	0.002	0.498	-1.797	<b>0.008</b>	-2.267	0.203
West	0.008	0.995	0.008	0.826	-0.090	0.536	-0.518	0.630

Significant values ( $P < 0.05$ ) are shown in bold.

### Potential distribution at LGM of the pollinators and *F. pumila* var. *pumila*

For *Wiebesia* sp. 1, *Wiebesia* sp. 2 and *F. pumila* var. *pumila*, the cross-validation of the climate envelope models revealed high mean model fitness for both LGM-CCSM and LGM-MIROC, and their current potential distribution ranges predicted by MAXENT were consistent with the records of current distribution (Fig. 3).

The highest climate suitability supported by both CCSM and MIROC showed two potential refugia for *Wiebesia* sp. 1, with the eastern refugium including the east coast and some islands in the Ryukyu Islands and the western refugium covering some areas in the mainland (Fig. 3b and c). The overlapped results from both models also detected that the potential refugia for *Wiebesia* sp. 2 comprised some areas in the south of mainland (the eastern refugium) and some island in South China Sea and Ryukyu Islands (the western refugium) (Fig. 3e and f). For *F. pumila* var. *pumila*, two potential refugia were found to cover most area of the potential refugia for the two cryptic pollinator species by both models: the eastern one contained the east coast area and some islands in the Ryukyu Islands and the western one covered a large area in the mainland (Fig. 3h and i).

## DISCUSSION

Both biotic and abiotic factors participate in shaping the phylogeographic patterns of organisms (Althoff *et al.* 2012; Hewitt 2000). Here, we sampled *F. pumila*

var. *pumila* and its host-specific pollinators across their distribution ranges in China to reveal their current genetic structure and postglacial phylogeographic history. Consistent with Chen *et al.* (2012), we found three cryptic pollinator species within our study area, with the dominant two species distributing in the northern and southern part of the distribution range of *F. pumila* var. *pumila* (Fig. 1a). The two dominant cryptic pollinator species and the plant displayed parallel current spatial genetic structure, with all species containing an eastern and a western genetic cluster (Fig. 1a and b). Furthermore, these three species had two potential glacial refugia, with the western refugium located in the mainland and the eastern refugium covering the coastal area and some nearby islands (Fig. 3), followed by expansion after the LGM (Fig. 2). These results suggest that these three species share similar phylogeographic history, contributing to the current parallel genetic structure. Therefore, our study provides evidence for our hypothesis that similar phylogeographic patterns appeared in the Last Glacial Period in these tightly interacting species.

The presence of three cryptic pollinator species and the absence of corresponding genetic divergences within *F. pumila* var. *pumila* indicate that the pollinators evolved at a faster rate than their host plant. As the key coevolved traits (e.g. attractive chemicals and body size) did not change among cryptic pollinator species (Wang *et al.* 2021), speciation within *W. pumilae* is possibly driven by abiotic factors rather than coevolution with *F. pumila*. Both the current distribution and the potential refugia

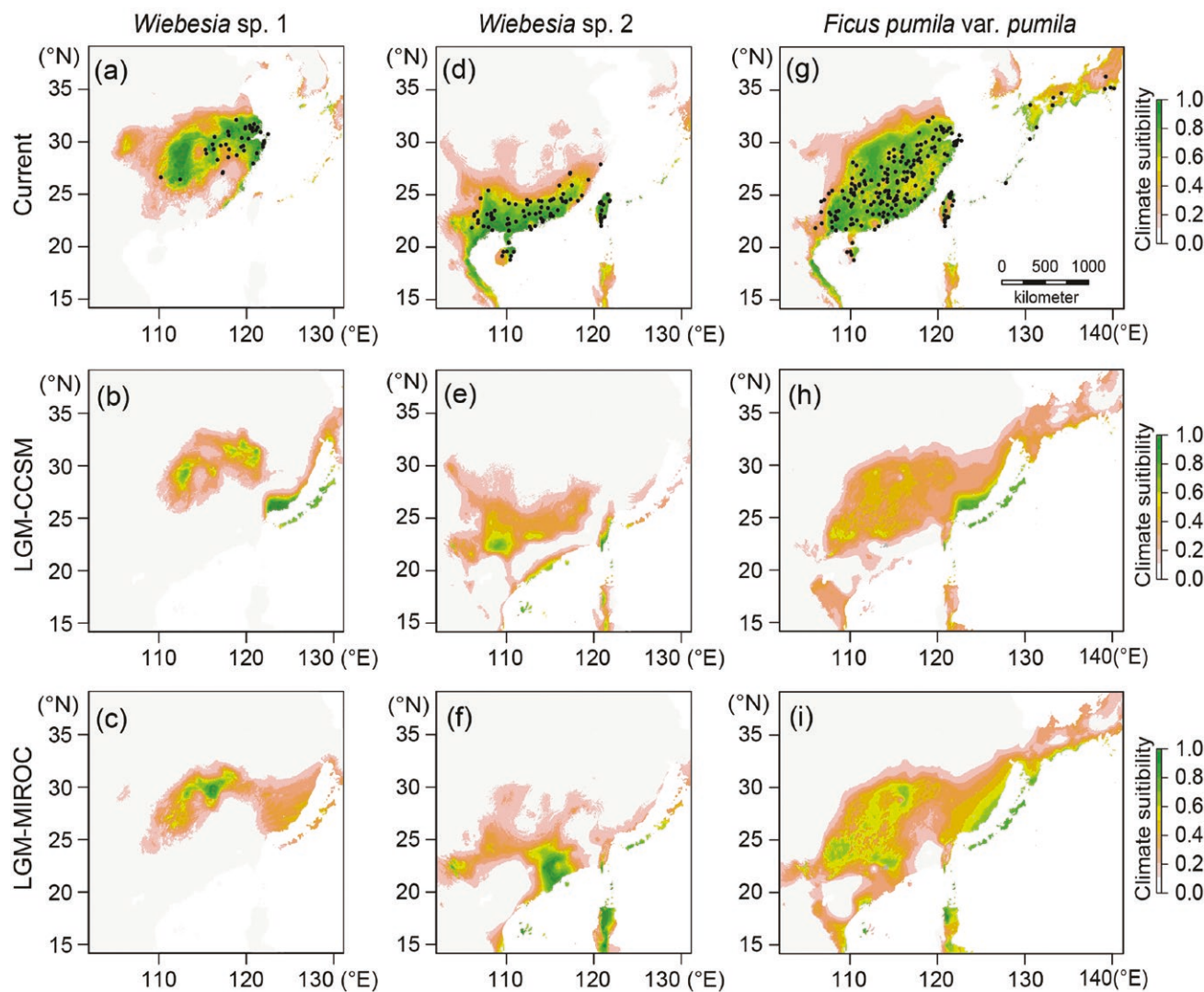


**Figure 3:** The current and LGM distribution of *Wiebesia* sp. 1 (a–c), *Wiebesia* sp. 2 (d–f) and *F. pumila* var. *pumila* (g–i) estimated by climate data from CCSM and MIROC model. The black dots are the locations with records of current distribution.

at LGM of *Wiebesia* sp. 1 are in the north of those of *Wiebesia* sp. 2, probably reflecting that *Wiebesia* sp. 1 adapts to the colder climate. *Wiebesia* sp. 3 is the only species pollinating *F. pumila* var. *awkeotsang* but only existed in a few *F. pumila* var. *pumila* populations. In addition, we did not find signals of postglacial expansion for this species. These suggest that it is a weaker competitor than other cryptic pollinator species, probably due to its later emergence during the flowering period of *F. pumila* (Liu *et al.* 2014). Nevertheless, source-sink dynamics has been found to assist the long-term maintenance of its island populations (Tong *et al.* 2021).

Consistent with Tian *et al.* (2015), which found identical genetic structure between two mutualists in another fig-pollinator mutualism, our results

showed roughly matched phylogeographic patterns between the pollinators and *F. pumila* var. *pumila*. This confirms that obligate pollinators should have synchronous responses with their host plants to changes in biogeographic factors. Nevertheless, slight differences were still observed between the pollinators and the plant, possibly due to the dispersal syndrome of *F. pumila* var. *pumila*.

Genetic structure of plant species is shaped by both pollen and seed dispersal (Wang *et al.* 2011), and the range expansion of the plants mainly relies on seed dispersal (Chen *et al.* 2008). Though pollen movements may play the predominant role in shaping the genetic structure of *F. pumila* var. *pumila* (reflected by the high pollen-to-seed dispersal ratio), frequent long-distance dispersal of *F. pumila* var.

*pumila* seeds is likely to occur because the common cpDNA haplotype (F1) in the eastern cluster also dominated some western populations (Fig. 1b). As an important food resource, mature figs of *F. pumila* can attract many long-distance seed dispersers (e.g. bats and large birds) (Corlett 2006). The presence of long-distance seed dispersal is likely to prevent genetic differentiation among *F. pumila* var. *pumila* populations pollinated by different cryptic pollinator species, resulting in a single eastern/western genetic cluster. Nevertheless, the Nanling–Wuyi Mountains may serve as a natural barrier for seed dispersal based on the cpDNA results.

Restricted movements of *W. pumilae* has been reported by Wang *et al.* (2013), and our study also detected isolation by distance patterns in *Wiebesia* sp. 1 and *Wiebesia* sp. 2 (Supplementary Fig. S3a–d), probably because of their extremely short lifespan at adult stage (1–3 days) (Liu *et al.* 2014). Thus, expansions of the pollinators from the coastal and insular refugia may not exactly keep pace with the colonization of *F. pumila* var. *pumila*, possibly resulting in a smaller range occupied by the eastern clusters of the pollinators than that occupied by the eastern cluster of *F. pumila* var. *pumila*. Moreover, the absence of geographic barriers between the two genetic clusters for either cryptic pollinator species indicates that the current genetic structure is not at equilibrium. The western cluster may be more adapted to mainland environments while coastal populations in the eastern clusters can get recruitment from island populations.

The presence of eastern and western potential refugia at LGM has been found in many species in the Sino–Japanese region, where the emergence of the land bridge of the East China Sea often acted as a corridor or a refugium during the Last Glacial Period (Jiang *et al.* 2021). However, this theory has seldom been tested for pairs of interacting species from different trophic levels. Our results provide evidence and support that tightly interacting insects can closely follow the migration trajectories of their host plants, offering an excellent case for understanding the historical dynamics of vertical diversity in East Asia. Moreover, consistent with other plant species in the Sino–Japanese region (e.g. Wang *et al.* 2015), the refugia in southwest mainland China harbored most genetic diversity of *F. pumila* var. *pumila*, as population genetic diversity of *F. pumila* var. *pumila* decreased with increasing latitude and longitude and a high haplotype diversity was found in the southwest of the plant's distribution range.

## CONCLUSIONS

Species in an ecosystem are inevitably linked by interspecific interactions, and the ongoing global changes are likely to distort these interactions and thus threaten the maintenance of biodiversity (Segar *et al.* 2020; Urban *et al.* 2016). Our results show that tightly interacting species responded similarly to historical climate changes, providing insights into the processes forming the current distribution of vertical diversity across different trophic levels.

### Supplementary Material

Supplementary material is available at *Journal of Plant Ecology* online.

Table S1: Population information of *F. pumila*.

Table S2: Outgroups used in the phylogenetic tree of fig wasps.

Table S3: Population information of *Wiebesia* sp. 1.

Table S4: Population information of *Wiebesia* sp. 2.

Table S5: Population information of *Wiebesia* sp. 3.

Figure S1: Results of genetic clustering for *Wiebesia pumilae* (*Wiebesia* spp.) (a) and its three cryptic species in *W. pumilae* (b–d) and *F. pumila* (e) using STRUCTURE.

Figure S2: Relationships between genetic diversity indices ( $N_A$ ,  $A_R$ ,  $H_E$ ,  $H_0$ ) in *F. pumila* populations and latitude (a–d) and longitude (e–h) using linear regressions.

Figure S3: Results of Mantel tests of the genetic divergence (represented by both  $F_{ST}/(1 - F_{ST})$  and  $F_{ST(ENA)}/(1 - F_{ST(ENA)})$ ) among populations of the three cryptic species in *W. pumilae* (a–f) and *F. pumila* (g, h) and the geographic distances (log-transformed) among populations.

### Authors' Contributions

Min Liu (Data curation, Formal analysis, Investigation, Methodology, Validation, Writing—original draft, Writing—review & editing), Man-Juan Huang (Formal analysis, Methodology, Validation, Visualization, Writing—review & editing), Finn Kjellberg (Conceptualization, Methodology, Writing—original draft, Writing—review & editing), Yan Chen (Data curation, Investigation, Methodology, Writing—review & editing), Jian Zhang (Data curation, Investigation, Methodology, Writing—review & editing), Yuan-Yuan Ding (Data curation, Investigation, Methodology, Writing—review & editing), Yang Yang (Data curation, Investigation, Methodology, Writing—review & editing), Jun-Yin Deng (Methodology, Writing—review & editing), Kai Jiang (Investigation, Methodology, Writing—review & editing), Yuan-Yuan Li (Investigation,

Methodology, Writing—review & editing), Xin Tong (Investigation, Methodology, Writing—review & editing), Tong Luo (Visualization, Writing—review & editing), Rong Wang (Conceptualization, Formal analysis, Investigation, Project administration, Supervision, Writing—review & editing), and Xiaoyong Chen (Conceptualization, Formal analysis, Funding acquisition, Investigation, Project administration, Resources, Supervision, Validation, Writing—original draft, Writing—review & editing)

### Funding

This study was supported by the National Natural Science Foundation of China (32171609, 32261123001) to X.-Y.C.

### Acknowledgements

Many local people provided support in field sample collection.

*Conflict of interest statement.* The authors declare that they have no conflict of interest.

## REFERENCES

Akesson A, Curtsdotter A, Eklöf A, *et al.* (2021) The importance of species interactions in eco-evolutionary community dynamics under climate change. *Nat Commun* **12**:4759. <https://doi.org/10.1038/s41467-021-24977-x>

Althoff DM, Segraves KA, Smith CI, *et al.* (2012) Geographic isolation trumps coevolution as a driver of yucca and yucca moth diversification. *Mol Phylogenet Evol* **62**:898–906. <https://doi.org/10.1016/j.ympev.2011.11.024>

Bansal M, Morley RJ, Nagaraju SK, *et al.* (2022) Southeast Asian Dipterocarp origin and diversification driven by Africa–India floristic interchange. *Science* **375**:455–460. <https://doi.org/10.1126/science.abk2177>

Benjamini Y, Hochberg Y (1995) Controlling the false discovery rate: a practical and powerful approach to multiple testing. *J R Stat Soc Ser B: Stat Method* **57**:289–300. <https://doi.org/10.1111/j.2517-6161.1995.tb02031.x>

Bothma JC, Matthee S, Matthee CA (2021) Comparative phylogeography between parasitic sucking lice and their host the Namaqua rock mouse, *Micaelamys namaquensis* (Rodentia: Muridae). *Zool J Linn Soc* **192**:1017–1028. <https://doi.org/10.1093/zoolinnean/zlaa122>

Chapuis MP, Estoup A (2007) Microsatellite null alleles and estimation of population differentiation. *Mol Biol Evol* **24**:621–631. <https://doi.org/10.1093/molbev/msl191>

Chen XY, Fan XX, Hu XS (2008) Roles of seed and pollen dispersal in natural regeneration of *Castanopsis fargesii* (Fagaceae): implications for forest management. *For Ecol Manage* **256**:1143–1150. <https://doi.org/10.1016/j.foreco.2008.06.014>

Chen Y, Compton SG, Liu M, *et al.* (2012) Fig trees at the northern limit of their range: the distributions of cryptic pollinators indicate multiple glacial refugia. *Mol Ecol* **21**:1687–1701. <https://doi.org/10.1111/j.1365-294X.2012.05491.x>

Clement M, Posada D, Crandall KA (2000) TCS: a computer program to estimate gene genealogies. *Mol Ecol* **9**:1657–1659. <https://doi.org/10.1046/j.1365-294x.2000.01020.x>

Collins WD, Bitz CM, Blackmon ML, *et al.* (2006) The Community Climate System Model version 3 (CCSM3). *J Climate* **19**:2122–2143. <https://doi.org/10.1175/JCLI3761.1>

Corlett RT (2006) Figs (*Ficus*, Moraceae) in urban Hong Kong, South China. *Biotropica* **38**:116–121. <https://doi.org/10.1111/j.1744-7429.2006.00109.x>

Cruaud A, Rønsted N, Chantarasuwan B, *et al.* (2012) An extreme case of plant-insect codiversification: figs and fig-pollinating wasps. *Syst Biol* **61**:1029–1047. <https://doi.org/10.1093/sysbio/sys068>

Deng JY, Fu RH, Compton SG, *et al.* (2020) Sky islands as foci for divergence of fig trees and their pollinators in southwest China. *Mol Ecol* **29**:762–782. <https://doi.org/10.1111/mec.15353>

Deng X, Liao Y, Wong D-M, *et al.* (2023) The genetic structuring in pollinating wasps of *Ficus hispida* in continental Asia. *Ecol Evol* **13**:e10518. <https://doi.org/10.1002/ece3.10518>

Després L, Pettex E, Plaisance V, *et al.* (2002) Speciation in the globeflower fly *Chiastocheta* spp. (Diptera: Anthomyiidae) in relation to host plant species, biogeography, and morphology. *Mol Phylogenet Evol* **22**:258–268. <https://doi.org/10.1006/mpev.2001.1047>

Drummond AJ, Suchard MA, Xie D, *et al.* (2012) Bayesian phylogenetics with BEAUTi and the BEAST 1.7. *Mol Biol Evol* **29**:1969–1973. <https://doi.org/10.1093/molbev/mss075>

Ennos RA (1994) Estimating the relative rates of pollen and seed migration among plant populations. *Heredity* **72**:250–259. <https://doi.org/10.1038/hdy.1994.35>

Espíndola A, Carstens BC, Alvarez N (2014) Comparative phylogeography of mutualists and the effect of the host on the genetic structure of its partners. *Biol J Linn Soc Lond* **113**:1021–1035. <https://doi.org/10.1111/bij.12393>

Evanno G, Regnaut S, Goudet J (2005) Detecting the number of clusters of individuals using the software STRUCTURE: a simulation study. *Mol Ecol* **14**:2611–2620. <https://doi.org/10.1111/j.1365-294X.2005.02553.x>

Excoffier L (2004) Patterns of DNA sequence diversity and genetic structure after a range expansion: lessons from the infinite-island model. *Mol Ecol* **13**:853–864. <https://doi.org/10.1046/j.1365-294x.2003.02004.x>

Excoffier L, Lischer HEL (2010) Arlequin suite ver 3.5: a new series of programs to perform population genetics analyses under Linux and Windows. *Mol Ecol Resour* **10**:564–567. <https://doi.org/10.1111/j.1755-0998.2010.02847.x>

Fu YX (1997) Statistical tests of neutrality of mutations against population growth, hitchhiking and background selection. *Genetics* **147**:915–925. <https://doi.org/10.1093/genetics/147.2.915>

Fu SY, Chen X, Wang KB, *et al.* (2024) Shared phylogeographic patterns and environmental responses of co-distributed soybean pests: insights from comparative phylogeographic studies of *Riptortus pedestris* and *Riptortus linearis* in the subtropics of East Asia. *Mol Phylogenet Evol* **195**:108055. <https://doi.org/10.1016/j.ympev.2024.108055>

Garrick RC, Nason JD, Fernández-Manjarrés JF, *et al.* (2013) Ecological coassociations influence species' responses to past

climatic change: an example from a Sonoran Desert bark beetle. *Mol Ecol* **22**:3345–3361. <https://doi.org/10.1111/mec.12318>

Godsoe W, Yoder JB, Smith CI, et al. (2008) Coevolution and divergence in the Joshua tree/yucca moth mutualism. *Am Nat* **171**:816–823. <https://doi.org/10.1086/587757>

Goudet J (1995) FSTAT (version 1.2): a computer program to calculate *F*-statistics. *J Hered* **86**:485–486. <https://doi.org/10.1093/oxfordjournals.jhered.a111627>

Guindon S, Dufayard JF, Lefort V, et al. (2010) New algorithms and methods to estimate maximum-likelihood phylogenies: assessing the performance of PhyML 3.0. *Syst Biol* **59**:307–321. <https://doi.org/10.1093/sysbio/syq010>

Hasumi H, Emori S (2004) *K-I Coupled GCM (MIROC) Description*. Tokyo, Japan: The University of Tokyo.

Hewitt G (2000) The genetic legacy of the Quaternary ice ages. *Nature* **405**:907–913. <https://doi.org/10.1038/35016000>

Jiang K, Tong X, Ding YQ, et al. (2021) Shifting roles of the East China Sea in the phylogeography of red nanmu in East Asia. *J Biogeogr* **48**:2486–2501. <https://doi.org/10.1111/jbi.14215>

Jiang K, Xiao YE, Gaitán-Espitia JD, et al. (2024) Multiple glacial refugia during Pleistocene climatic oscillations shape the genetic pattern of *Machilus thunbergii* across East Asia. *Biol J Linn Soc* **143**:blae082. <https://doi.org/10.1093/biolinnean/blae082>

Kephart S, Reynolds RJ, Rutter MT, et al. (2006) Pollination and seed predation by moths on *Silene* and allied Caryophyllaceae: evaluating a model system to study the evolution of mutualisms. *New Phytol* **169**:667–680. <https://doi.org/10.1111/j.1469-8137.2005.01619.x>

Kreger KM, Shaban B, Wapstra E, et al. (2020) Phylogeographic parallelism: concordant patterns in closely related species illuminate underlying mechanisms in the historically glaciated Tasmanian landscape. *J Biogeogr* **47**:1674–1686. <https://doi.org/10.1111/jbi.13831>

Lan B, Hu X, Wang Y, et al. (2022) The abundance effect on network nestedness is stronger for parasitic than herbivory interactions. *J Plant Ecol* **15**:1133–1141. <https://doi.org/10.1093/jpe/rta052>

Librado P, Rozas J (2009) DnaSP v5: a software for comprehensive analysis of DNA polymorphism data. *Bioinformatics* **25**:1451–1452. <https://doi.org/10.1093/bioinformatics/btp187>

Lin RC, Yeung CKL, Li SH (2008) Drastic post-LGM expansion and lack of historical genetic structure of a subtropical fig-pollinating wasp (*Ceratosolen* sp. 1) of *Ficus septica* in Taiwan. *Mol Ecol* **17**:5008–5022. <https://doi.org/10.1111/j.1365-294X.2008.03983.x>

Liu M, Zhang J, Chen Y, et al. (2013) Contrasting genetic responses to population fragmentation in a coevolving fig and fig wasp across a mainland–island archipelago. *Mol Ecol* **22**:4384–4396. <https://doi.org/10.1111/mec.12406>

Liu M, Zhao R, Chen Y, et al. (2014) Competitive exclusion among fig wasps achieved via entrainment of host plant flowering phenology. *PLoS One* **9**:e97783. <https://doi.org/10.1371/journal.pone.0097783>

Liu M, Compton SG, Peng FE, et al. (2015) Movements of genes between populations: are pollinators more effective at transferring their own or plant genetic markers? *Proc Biol Sci* **282**:20150290. <https://doi.org/10.1098/rspb.2015.0290>

Lu LM, Mao LF, Yang T, et al. (2018) Evolutionary history of the angiosperm flora of China. *Nature* **554**:234–238. <https://doi.org/10.1038/nature25485>

Magalhaes IS, Gleiser G, Labouche AM, et al. (2011) Comparative population genetic structure in a plant-pollinator/seed predator system. *Mol Ecol* **20**:4618–4630. <https://doi.org/10.1111/j.1365-294X.2011.05296.x>

Maron JL, Agrawal AA, Schemske DW (2019) Plant-herbivore coevolution and plant speciation. *Ecology* **100**:e02704. <https://doi.org/10.1002/ecy.2704>

Marske KA, Thomaz AT, Knowles LL (2020) Dispersal barriers and opportunities drive multiple levels of phylogeographic concordance in the Southern Alps of New Zealand. *Mol Ecol* **29**:4665–4679. <https://doi.org/10.1111/mec.15655>

Naimi B, Hamm NAS, Groe TA, et al. (2014) Where is positional uncertainty a problem for species distribution modelling? *Ecography* **37**:191–203. <https://doi.org/10.1111/j.1600-0587.2013.00205.x>

Oksanen J, Blanchet FG, Friendly M, et al. (2019) *vegan: Community Ecology Package*. R Package Version 2.5-6. <https://CRAN.R-project.org/package=vegan> (20 September 2019, date last accessed).

Peakall R, Smouse PE (2012) GenAlEx 6.5: genetic analysis in Excel. Population genetic software for teaching and research—an update. *Bioinformatics* **28**:2537–2539. <https://doi.org/10.1093/bioinformatics/bts460>

Phillips SJ, Dudik M (2008) Modeling of species distributions with Maxent: new extensions and a comprehensive evaluation. *Ecography* **31**:167–175. <https://doi.org/10.1111/j.0906-7590.2007.5203.x>

Pritchard JK, Stephens M, Donnelly P (2000) Inference of population structure using multilocus genotype data. *Genetics* **155**:945–959. <https://doi.org/10.1093/genetics/155.2.945>

Rambaut A, Drummond AJ, Xie D, et al. (2018) Posterior summarisation in Bayesian phylogenetics using Tracer 1.7. *Syst Biol* **67**:901–904. <https://doi.org/10.1093/sysbio/syy032>

Rodriguez LJ, Bain A, Chou LS, et al. (2017) Diversification and spatial structuring in the mutualism between *Ficus septica* and its pollinating wasps in insular South East Asia. *BMC Evol Biol* **17**:207. <https://doi.org/10.1186/s12862-017-1034-8>

Rousset F (2008) GENEPOP'007: a complete re-implementation of the GENEPOP software for Windows and Linux. *Mol Ecol Resour* **8**:103–106. <https://doi.org/10.1111/j.1471-8286.2007.01931.x>

Segar ST, Fayle TM, Srivastava DS, et al. (2020) The role of evolution in shaping ecological networks. *Trends Ecol Evol* **35**:454–466. <https://doi.org/10.1016/j.tree.2020.01.004>

Slatkin M, Hudson RR (1991) Pairwise comparisons of mitochondrial DNA sequences in stable and exponentially growing populations. *Genetics* **129**:555–562. <https://doi.org/10.1093/genetics/129.2.555>

Tajima F (1989) Statistical method for testing the neutral mutation hypothesis by DNA polymorphism. *Genetics* **123**:585–595. <https://doi.org/10.1093/genetics/123.3.585>

Tamura K, Stecher G, Peterson D, *et al.* (2013) MEGA6: molecular evolutionary genetics analysis version 6.0. *Mol Biol Evol* **30**:2725–2729. <https://doi.org/10.1093/molbev/mst197>

Thrall PH, Hochberg ME, Burdon JJ, *et al.* (2007) Coevolution of symbiotic mutualists and parasites in a community context. *Trends Ecol Evol* **22**:120–126. <https://doi.org/10.1016/j.tree.2006.11.007>

Tian EW, Nason JD, Machado CA, *et al.* (2015) Lack of genetic isolation by distance, similar genetic structuring but different demographic histories in a fig-pollinating wasp mutualism. *Mol Ecol* **24**:5976–5991. <https://doi.org/10.1111/mec.13438>

Tong X, Ding YY, Deng JY, *et al.* (2021) Source-sink dynamics assists the maintenance of a pollinating wasp. *Mol Ecol* **30**:4695–4707. <https://doi.org/10.1111/mec.16104>

Tong X, Li JH, Jiang K, *et al.* (2022) Back to the brink: phylogeography and demographic history of the endangered *Torreya jackii*. *J System Evol* **60**:1158–1171. <https://doi.org/10.1111/jse.12728>

Urban MC, Bocedi G, Hendry AP, *et al.* (2016) Improving the forecast for biodiversity under climate change. *Science* **353**:aad8466. <https://doi.org/10.1126/science.aad8466>

van Oosterhout C, Hutchinson WF, Wills DPM, *et al.* (2004) MICRO-CHECKER: software for identifying and correcting genotyping errors in microsatellite data. *Mol Ecol Notes* **4**:535–538. <https://doi.org/10.1111/j.1471-8286.2004.00684.x>

Verbruggen H (2012) *OccurrenceThinner* version 1.04. <https://github.com/hverbruggen/OccurrenceThinner> (25 September 2019, date last accessed).

Wang R, Compton SG, Chen XY (2011) Fragmentation can increase spatial genetic structure without decreasing pollen-mediated gene flow in a wind-pollinated tree. *Mol Ecol* **20**:4421–4432. <https://doi.org/10.1111/j.1365-294X.2011.05293.x>

Wang HY, Hsieh CH, Huang CG, *et al.* (2013) Genetic and physiological data suggest demographic and adaptive responses in complex interactions between populations of figs (*Ficus pumila*) and their pollinating wasps (*Wiebeisia pumilae*). *Mol Ecol* **22**:3814–3832. <https://doi.org/10.1111/mec.12336>

Wang YH, Jiang WM, Comes HP, *et al.* (2015) Molecular phylogeography and ecological niche modelling of a widespread herbaceous climber, *Tetrastigma hemsleyanum* (Vitaceae): insights into Plio-Pleistocene range dynamics of evergreen forest in subtropical China. *New Phytol* **206**:852–867. <https://doi.org/10.1111/nph.13261>

Wang R, Chen XY, Chen Y, *et al.* (2019) Loss of top-down biotic interactions changes the relative benefits for obligate mutualists. *Proc Biol Sci* **286**:20182501. <https://doi.org/10.1098/rspb.2018.2501>

Wang R, Yang Y, Jing Y, *et al.* (2021) Molecular mechanisms of mutualistic and antagonistic interactions in a plant-pollinator association. *Nat Ecol Evol* **5**:974–986. <https://doi.org/10.1038/s41559-021-01469-1>

Wang AY, Peng YQ, Cook JM, *et al.* (2023) Host insect specificity and interspecific competition drive parasitoid diversification in a plant-insect community. *Ecology* **104**:e4062. <https://doi.org/10.1002/ecy.4062>

Weiblen GD (2002) How to be a fig wasp. *Annu Rev Entomol* **47**:299–330. <https://doi.org/10.1146/annurev.ento.47.091201.145213>

Xu L, Harrison RD, Yang P, *et al.* (2011) New insight into the phylogenetic and biogeographic history of genus *Ficus*: vicariance played a relatively minor role compared with ecological opportunity and dispersal. *J Syst Evol* **49**:546–557. <https://doi.org/10.1111/j.1759-6831.2011.00155.x>

Yang LY, Machado CA, Dang XD, *et al.* (2015) The incidence and pattern of copollinator diversification in dioecious and monoecious figs. *Evolution* **69**:294–304. <https://doi.org/10.1111/evo.12584>

Yang Y, Zhang YY, Zhang Y, *et al.* (2023) Selection to attract pollinators and to confuse antagonists specializes fig-pollinator chemical communications. *J System Evol* **61**:454–464. <https://doi.org/10.1111/jse.12908>

Yin BF, Zhang YM, Zhang HX, *et al.* (2023) Phylogeographic structure of *Syntrichia caninervis* Mitt, a xerophytic moss, highlights the expanded during glacial period. *J Plant Ecol* **16**:rtac057. <https://doi.org/10.1093/jpe/rtac057>

Yu H, Nason JD (2013) Nuclear and chloroplast DNA phylogeography of *Ficus hirta*: obligate pollination mutualism and constraints on range expansion in response to climate change. *New Phytol* **197**:276–289. <https://doi.org/10.1111/j.1469-8137.2012.04383.x>

Yu H, Tian EW, Zheng LN, *et al.* (2019) Multiple parapatric pollinators have radiated across a continental fig tree displaying clinal genetic variation. *Mol Ecol* **28**:2391–2405. <https://doi.org/10.1111/mec.15046>

Zhang J, Jiang K, Shi YS, *et al.* (2011) Development and polymorphism of microsatellite primers in *Ficus pumila* L. (Moraceae). *Am J Bot* **98**:e170–e172. <https://doi.org/10.3732/ajb.1000340>

Zhang Q, Tong X, Li YY, *et al.* (2022) Presence of cryptic species in host insects forms a hierarchical *Wolbachia* infection pattern. *Entomol Gen* **42**:571–578. <https://doi.org/10.1127/entomologia/2022/1392>